Inorg. Chem. **2002**, *41*, 4033–4043

Synthesis and Structural, Spectroscopic, and Electrochemical Characterization of New Ruthenium Dimethyl Sulfoxide Nitrosyls

Barbara Serli,[†] Ennio Zangrando,[†] Elisabetta Iengo,[†] Giovanni Mestroni,[†] Lesley Yellowlees,[‡] and Enzo Alessio*,[†]

Dipartimento di Scienze Chimiche, Università di Trieste, 34127 Trieste, Italy, and Department of Chemistry, University of Edinburgh, Edinburgh EH9 3JJ, U.K.

Received December 18, 2001

The reactivity of ruthenium(II)– and ruthenium(III)–chloride–dimethyl sulfoxide precursors and of the antimetasatic drug [ImH][*trans*-$RuCl_4$(dmso-S)(Im)] (NAMI-A, Im = imidazole, dmso = dimethyl sulfoxide) toward NO was investigated. Treatment of [$(dmso)_2$H][*trans*-$RuCl_4$(dmso-$S)_2$] and *mer*-$RuCl_3(dmso)_3$ with gaseous NO yielded [$(dmso)_2$H][*trans*-$RuCl_4$(dmso-O)(NO)] (**1**) and *mer,cis*-$RuCl_3$(dmso-$O)_2$(NO) (**2**), respectively. Thus, coordination of the strong π-acceptor NO induces a S to O linkage isomerization of the dmso trans to it to avoid competition for π-electrons. In light-protected nitromethane solutions, complex **2** equilibrates slowly with the two isomers *mer*-$RuCl_3$(dmso-S)(dmso-O)(NO) (**3**), with NO trans to Cl, and *mer*-$RuCl_3$(dmso-S)(dmso-O)(NO) (**4**), with NO trans to dmso-O; the equilibrium mixture consists of ca. 64% **2**, 3% **3**, and 33% **4**. Treatment of the Ru(II) precursor *trans*-$RuCl_2$(dmso-$S)_4$ with gaseous NO in CH_2Cl_2 solution yielded the nitrosyl–nitro derivative *trans*,*cis*,*cis*-$RuCl_2$-(dmso-$O)_2$(NO)(NO_2) (**5**). Finally, [$(Im)_2$H][*trans*-$RuCl_4$(Im)(NO)] (**6**) was prepared by treatment of [ImH][*trans*-$RuCl_4$-(dmso-O)(NO)] (**1Im**) with an excess of imidazole in refluxing acetone. The spectroscopic features are consistent with the $\{Ru(NO)\}^6$ formulation for all complexes, that is, a diamagnetic Ru^{II} nucleus bound to NO^+. Compounds **1**, **2**, **5**, and **6** were characterized also by X-ray crystallography; they all show a linear nitrosyl group, with short Ru–NO bond distances consistent with a strong $d_\pi \rightarrow \pi^*$ NO back-bonding. An unusual inertness of O-bonded dmso was observed in compound **1**. Complexes **1**, **2**, **3**, **5**, and **6** are all redox active in DMF solutions showing irreversible reductions whose peak potentials depend on the other ligands attached to the Ru metal center. The site of reduction is the NO^+ moiety. The reduced complexes are not stable and release a Cl^- or NO_2^- ligand followed by the $NO^\bullet$ radical. The chemical reactions following electron transfer are all fast (rate constant >100 s^{-1} at 293 K). The Ru product species are not redox active within the DMF window.

Introduction

In recent years, we showed that several ruthenium(II)−and ruthenium(III)−dimethyl sulfoxide (dmso) complexes, that are not cytotoxic in vitro, are endowed with anticancer activity against animal tumor models.[1] Some of the ruthenium compounds developed by us, while not particularly active against the growth of primary tumor, are very effective in selectively inhibiting the formation and growth of spontaneous metastases.[2] The antimetastatic activity of one such compound, [ImH][*trans*-$RuCl_4$(dmso-S)(Im)] (NAMI-A, Im = imidazole), in preclinical tests was so remarkable that in 1999 it was introduced into phase I clinical trials.

The low cytotoxicity of NAMI-A and related Ru−dmso complexes suggests that their primary mechanism of action is different from that of cytostatic Pt drugs and might be unrelated to interactions with DNA.[3]

One possibility for explaining the activity of NAMI-A against disseminated tumors is that it interferes with NO metabolism in vivo. Nitric oxide is known to play an important role in many biological functions,[4] and recently, it was demonstrated to be involved as mediator in one tumor-induced angiogenic process, which is a key step in the

* To whom correspondence should be addressed. E-mail: alessi@univ.trieste.it. Phone: +39 040 5583961. Fax: +39 040 5583903.
[†] Università di Trieste.
[‡] University of Edinburgh.

(1) Sava, G.; Alessio, E.; Bergamo, A.; Mestroni, G. In *Topics in Biological Inorganic Chemistry, Volume 1: Metallo-pharmaceuticals*; Clarke, M. J, Sadler, P. J., Eds.; Springer: Berlin, 1999; pp 143−169.
(2) Sava, G.; Gagliardi, R.; Bergamo, A.; Alessio, E.; Mestroni, G. *Anticancer Res.* **1999**, *19*, 969−972.
(3) Zorzet, S.; Bergamo, A.; Cocchietto, M.; Sorc, A.; Gava, B.; Alessio, E.; Iengo, E.; Sava, G. *J. Pharmacol. Expl. Ther.* **2000**, *295*, 927−933.
(4) (a) Murad, F. *Angew. Chem., Int. Ed.* **1999**, *38*, 1856−1868. (b) Furchgott, R. F. *Angew. Chem., Int. Ed.* **1999**, *38*, 1871−1880. (c) Ignarro, I. J. *Angew. Chem., Int. Ed.* **1999**, *38*, 1882−1892.

10.1021/ic011291v CCC: $22.00
Published on Web 07/03/2002

formation of metastases.[5] NO is also known to interact in vivo with iron proteins;[6] thus, ruthenium action might also occur through an iron-mimicking mechanism.

By virtue of the well documented affinity of ruthenium for NO,[7] several compounds of this metal are being investigated as NO scavengers (e.g., for the treatment of septic shock);[8] on the other hand, ruthenium nitrosyl complexes are investigated as controlled NO-releasing agents for medicinal applications,[9,10] such as the control of high blood pressure (vasodilatation). Ruthenium−NO complexes are also investigated as potential antitumor agents: if the release of cytotoxic NO might be induced to occur within tumor cells, it would lead to cell death.

Most octahedral ruthenium nitrosyls feature the linear $\{Ru^{II}(NO^{+})\}^6$ moiety;[11] NO release can be induced by one-electron reduction,[9] which occurs at the NO^+ to yield coordinated $NO^{\bullet}$, or by photolysis (photodynamic therapy).[10,12] In general, it has been found that the Ru−NO bond strength, and consequently the rate of NO release, depends markedly on the π-acceptor strength of the ligand coordinated trans to it.[9]

Within this general framework, we decided to investigate the reactivity of basic ruthenium−chloride−dmso complexes and of NAMI-A toward NO with the aim of producing spectroscopically and structurally well characterized models to be used as reference compounds in subsequent biomimetic studies.

Despite the large number of ruthenium nitrosyl compounds described in the literature,[13−22] the examples involving sulfoxide derivatives are very few. The first dates back to 1973, when Wilkinson and co-workers reported that treatment of $RuCl_3$ with NO in dmso solution yielded a complex formulated as $RuCl_3(dmso)_2(NO)$ on the basis of elemental analysis;[23] the same complex was later described by Fergusson and co-workers, together with IR evidence indicating a linear Ru−NO system and sulfoxide coordination through oxygen.[24] The same group described the crystal structures of *mer*-$RuBr_3(NO)(Et_2S)(Et_2SO)$ and of the dinuclear di-μ-bromo complex $[Ru(NO)Br_3(Et_2SO)]_2$), in which the diethylsulfoxide is bound through oxygen trans to linear NO.[25] To date, these two examples represented the only structural characterizations available for ruthenium−sulfoxide nitrosyl complexes. In this paper, we report on the synthesis and spectroscopic, structural, and electrochemical characterization of several new Ru−dmso nitrosyls, derived from both ruthenium(II)− and ruthenium(III)−chloride−dimethyl sulfoxide precursors.

Experimental Section

Materials. Hydrated $RuCl_3$ was a loan from Johnson Matthey. $[(dmso)_2H][trans\text{-}RuCl_4(dmso\text{-}S)_2]$,[26] *mer*-$RuCl_3(dmso)_3$,[26] *cis*-$RuCl_2(dmso)_4$,[27] and *trans*-$RuCl_2(dmso\text{-}S)_4$[27] were prepared according to literature procedures. $[ImH][trans\text{-}RuCl_4(dmso\text{-}S)_2]$ was prepared by treatment of $[(dmso)_2H][trans\text{-}RuCl_4(dmso\text{-}S)_2]$ with a 2-fold excess of imidazolium chloride in an ethanol/water mixture (98.5/1.5). Nitric oxide was generated by dripping concentrated sulfuric acid onto $NaNO_2$, passing it through a saturated aqueous solution of NaOH, and then bubbling through the solution/suspension. UV−vis spectra were obtained on a Jasco V-550 spectrometer in quartz cells. ^{1}H NMR and ^{13}C NMR spectra were recorded at 400 and 100.5 MHz, respectively, on a JEOL Eclipse 400 FT instrument. All spectra were run at room temperature unless differently stated. Proton peak positions were referenced to sodium2,2-dimethyl-2-silapentane-5-sulfonate (DSS) in D_2O and to the peak of residual nondeuterated solvent set at 4.33 ppm in CD_3NO_2. Carbon peak positions were referenced to the central peak of nitromethane set at 62.8 ppm. Infrared spectra were recorded on a Perkin-Elmer 983G spectrometer. Elemental analysis (C, H, N) was performed by Dr. E. Cebulec at the Dipartimento di Scienze Chimiche, Università di Trieste.

Synthesis of the Complexes. $[(dmso)_2H][trans\text{-}RuCl_4(dmso\text{-}O)(NO)]$ (1). The preparation of **1** could be perfomed from $[(dmso)_2H][trans\text{-}RuCl_4(dmso\text{-}S)_2]$ either in nitromethane (path a)

(5) Ziche, M.; Morbidelli, L.; Choudhri, R.; Zhang, H.-T.; Donnini, S.; Granger, H. J.; Bicknell, R. *J. Clin. Invest.* **1997**, *99*, 2625−2634.
(6) Pfeiffer, S.; Mayer, B.; Hemmens, B. *Angew. Chem., Int. Ed.* **1999**, *38*, 1714−1731.
(7) Richter-Addo, G. B.; Leggdins, P. In *Metal Nitrosyls*; Oxford University Press: New York, 1992
(8) (a) Fricker, S. P. *Platinum Met. Rev.* **1995**, *39*, 150−159. (b) Wilson, M. T.; Slade, E.; Fricker, S. P.; Murrer, B. A.; Powell, N. A.; Henderson, G. R. *Chem. Commun.* **1997**, 47−48. (c) Chen, Y.; Shepherd, R. E. *J. Inorg. Biochem.* **1997**, *68*, 183−193. (d) Chen, Y.; Lin. F.-T.; Shepherd, R. E. *Inorg. Chem.* **1999**, *38*, 973−983. (e) Marmion, C. J.; Murphy, T.; Docherty, J. R.; Nolan, K. B. *Chem. Commun.* **2000**, 1153−1154.
(9) (a) Lang, D. R.; Davis, J. A.; Lopes, L. G. F.; Ferro, A. A.; Vasconcellos, L. C. G.; Franco, D. W.; Tfouni, E.; Wieraszko, A.; Clarke, M. J. *Inorg. Chem.* **2000**, *39*, 2294−2300. (b) Lopes, L. G. F.; Wieraszko, A.; El-Sherif, Y.; Clarke, M. J. *Inorg. Chim. Acta* **2001**, *312*, 15−22.
(10) (a) Slocik, J. M.; Shepherd, R. E. *Inorg. Chim. Acta* **2000**, *311*, 80−94. (b) Slocik, J. M.; Ward, M. S.; Somayajula, K. V.; Shepherd, R. E. *Transition Met. Chem.* **2001**, *26*, 351−364.
(11) Wescott, B. L.; Enemark, J. H. In *Inorganic Electronic Structure and Spectroscopy, Volume II: Applications and Case Studies*; Solomon, E. I., Lever, A. B. P., Eds.; John Wiley & Sons: New York, 1999; pp 403−450.
(12) The term "caged NO" has been adopted by the biomedical community involved in the photodynamic therapy to designate the $\{Ru^{II}(NO^{+})\}^6$ nitrosyl $[RuCl_3(NO)(H_2O)_2]$.
(13) Zarhoule, R.; Duc, G.; Deloume, J. *Inorg. Chim. Acta* **1989**, *160*, 59−63.
(14) Coe, B. J.; Meyer, T. J.; White, P. S. *Inorg. Chem.* **1995**, *34*, 593−602.
(15) Ooyama, D.; Nagao, N.; Nagao, H.; Miura, Y.; Hasegawa, A.; Ando, K.; Howell, F. S.; Mukaida, M.; Tanaka, K. *Inorg. Chem.* **1995**, *34*, 6024−6033.
(16) Kadish, K. M.; Adamian, V. A.; Van Caemelbecke, E.; Tan, Z.; Tagliatesta, P.; Bianco, P.; Boschi, T.; Yi, G.; Khan, M. A.; Richter-Addo, G. B. *Inorg. Chem.* **1996**, *35*, 1343−1348.
(17) Bohle, D. S.; Hung, C.; Powell, A. K.; Smith, B. D.; Wocaldo, S. *Inorg. Chem.* **1997**, *36*, 1992−1993.
(18) Borges, S. da S. S.; Davanzo, C. U.; Castellano, E. E.; Z-Schpector, J.; Silva, S. C.; Franco, D. W. *Inorg. Chem.* **1998**, *37*, 2670−2677.
(19) Gomes, M. G.; Davanzo, C. U.; Silva, S. C.; Lopes, L. G.; Santos, P. S.; Franco, D. W. *J. Chem. Soc., Dalton Trans.* **1998**, 601−607.
(20) Nagao, H.; Ito, K.; Tsuboya, N.; Ooyama, D.; Nagao, N.; Howell, F. S.; Mukaida, M. *Inorg. Chim. Acta* **1999**, *290*, 113−119.
(21) Bezerra, C. W. B.; da Silva, S. C.; Gambardella, M. T. P.; Santos, R. H. A.; Plicas, L. M. A.; Tfouni, E.; Franco, D. W. *Inorg. Chem.* **1999**, *38*, 5660−5667.
(22) Bohle, D. S.; Sagan, E. S. *Eur. J. Inorg. Chem.* **2000**, 1609−1616.
(23) Evans, I. P.; Spencer, A.; Wilkinson, W. *J. Chem. Soc., Dalton Trans.* **1973**, 204−209.
(24) Coll, R. K.; Fergusson, J. E.; McKee, V.; Page, C. T.; Robinson, W. T.; Keong, T. S. *Inorg. Chem.* **1987**, *26*, 106−111.
(25) Fergusson, J. E.; Page, C. T.; Robinson, W. T. *Inorg. Chem.* **1976**, *15*, 2270−2273.
(26) Alessio, E.; Balducci, G.; Calligaris, M.; Costa, G.; Attia, W. M. *Inorg. Chem.* **1991**, *30*, 609−618.
(27) Alessio, E.; Mestroni, G.; Nardin, G.; Attia, W. M.; Calligaris, M.; Sava, G.; Zorzet, S. *Inorg. Chem.* **1988**, *27*, 4099−4106.

or in water (path b); alternatively, complex **1** could be prepared also directly from $RuCl_3$ (path c).

(a) A 0.5 g amount of $[(dmso)_2H][trans\text{-}RuCl_4(dmso\text{-}S)_2]$ (0.9 mmol) was partially dissolved in 10 mL of nitromethane; nitric oxide was bubbled through the mixture for 1.5 h, yielding a dark purple-red solution that was then evaporated to an oil. Addition of acetone (5 mL) induced the formation of a dark purple solid which was removed by filtration, washed with cold acetone and diethyl ether, and vacuum-dried. A further crop of product was obtained from the concentrated mother liquor upon addition of a small amount of diethyl ether. Yield: 0.30 g (65%). Anal. Calcd for $C_6H_{19}NCl_4O_4RuS_3$ (M_r 508.28): C, 14.2; H, 3.77; N, 2.76. Found: C, 14.3; H, 3.69; N, 2.82. ^{1}H NMR spectrum in D_2O: 2.71 ppm (12, s, free dmso), 2.95 (6, s, dmso-O). $^{13}C\{^1H\}$ NMR spectrum in D_2O: 41.7 ppm (dmso), 40.3 (dmso-O). Selected IR, cm^{-1} (KBr): $\nu_{N\equiv O}$ 1864 (vs), ν_{SO} 924 (vs) (dmso-O), 725 (s, v br) ($(dmso)_2H$), ν_{Ru-O} 501 (m). UV−vis spectrum (λ_{max}, nm (ϵ, M^{-1} cm^{-1})): in H_2O solution, 504 (v br) (60).

(b) A 0.3 g amount of $[(dmso)_2H][trans\text{-}RuCl_4(dmso\text{-}S)_2]$ (0.54 mmol) was dissolved in 5 mL of water; nitric oxide was bubbled through the solution for 30 min, yielding a dark purple-red solution that was then evaporated to an oil and treated as previously described. Yield: 0.12 g (44.4%). Anal. Calcd for $C_6H_{19}NCl_4O_4RuS_3$ (M_r 508.28): C, 14.2; H, 3.77; N, 2.76. Found: C, 14.1; H, 3.70; N, 2.80.

When the preparation of **1** was performed on larger amounts of precursor (≥1 g), a small amount of an orange precipitate, identified as neutral species $RuCl_3$(dmso-S)(dmso-O)(NO) (**3**), formed during the reaction (see later).

(c) A 1.1 g amount of $RuCl_3 \cdot 3H_2O$ (ca. 4.2 mmol) was refluxed for 3 h in 25 mL of ethanol; after cooling to room temperature, the deep-green solution was filtered over fine paper, and NO was bubbled for 6 h. Dimethyl sulfoxide (1 mL) and concentrated HCl (0.5 mL) were then added, and the solution was further refluxed for 45 min, turning purple-red. Concentration to ca. 2 mL and addition of acetone (7 mL) induced the formation of a microcrystalline dark purple solid, which was filtered, washed with cold acetone and diethyl ether, and vacuum-dried. A further crop of precipitate was obtained from the mother liquor upon addition of a few milliliters of diethyl ether. Total yield: 1.64 g (77%).

[ImH][*trans*-RuCl$_4$(dmso-O)(NO)] (1Im). A 0.5 g amount of $[ImH][trans\text{-}RuCl_4(dmso\text{-}S)_2]$ (1.07 mmol) was partially dissolved in 10 mL of nitromethane, and nitric oxide was bubbled through the system. Within 2 h, the starting material dissolved completely, and a dark purple-red solution was obtained. Nitromethane was rotary-evaporated and the resulting red oil redissolved in acetone (5 mL); a dark-pink precipitate formed rapidly and was removed by filtration, washed with cold acetone and diethyl ether, and vacuum-dried. Yield: 0.14 g (30%). Anal. Calcd for $C_5H_{11}N_3Cl_4O_2RuS$ (M_r 420.10): C, 14.3; H, 2.64; N, 10.00. Found: C, 14.1; H, 2.49; N, 10.20. ^{1}H NMR spectrum in D_2O: 2.97 ppm (6, s, dmso-O), 7.45 (2, s, ImH), 8.59 (1, s, ImH). Selected IR, cm^{-1} (KBr): $\nu_{N\equiv O}$ 1864 (vs), ν_{SO} 922 (vs) (dmso-O), (ImH) 1043 (s), 626 (s), ν_{Ru-O} 501 (m).

[TBA][*trans*-RuCl$_4$(dmso-O)(NO)] (1TBA). A 0.28 g amount (1 mmol) of tetra *n*-butylammonium (TBA) chloride dissolved in 1.4 mL of water was added to a solution of $[(dmso)_2H][trans\text{-}RuCl_4(dmso\text{-}O)(NO)]$ (**1**) (0.25 g, 0.5 mmol) in 2 mL of water. A dark-pink precipitate formed immediately and was removed by filtration, washed with water, cold acetone, and diethyl ether, and vacuum-dried. Yield: 0.22 g (75%). Anal. Calcd for $C_{18}H_{42}N_2Cl_4O_2RuS$ (M_r 593.48): C, 36.4; H, 7.13; N, 4.72. Found: C, 36.6; H, 7.21; N, 4.67. ^{1}H NMR spectrum in CD_3NO_2: 1.02 (12, t, TBA), 1.46 (8, m, TBA), 1.67 (8, m, TBA), 3.25 (8, m, TBA), 2.91 ppm (6, s, dmso-O). Selected IR, cm^{-1} (KBr): $\nu_{N\equiv O}$ 1867 (vs), ν_{SO} 937 (vs) (dmso-O), ν_{Ru-O} 492 (m). UV−vis spectrum (λ_{max}, nm (ϵ, M^{-1} cm^{-1})): in CH_3NO_2 solution, 508 (v br) (55).

***mer,cis*-RuCl$_3$(dmso-O)$_2$(NO) (2).** A 0.3 g amount of *mer*-$RuCl_3(dmso)_3$ (0.68 mmol) was dissolved in 6 mL of CH_2Cl_2, and nitric oxide was bubbled through the solution for 2 h, causing the system to turn dark purple-red. A solid of the same color, whose precipitation became apparent after ca. 1 h, was collected by filtration, washed with dichloromethane and diethyl ether, and vacuum-dried. Yield: 0.18 g (66%). Anal. Calcd for $C_4H_{12}NCl_3O_3RuS_2$ (M_r 393.69): C, 12.2; H, 3.08; N, 3.56. Found: C, 12.1; H, 2.97; N, 3.58. ^{1}H NMR spectrum in CD_3NO_2: 2.88 (6, s, dmso-O), 2.96 (6, s, dmso-O). $^{13}C\{^1H\}$ NMR spectrum in CD_3NO_2: 38.5 (dmso-O). Selected IR, cm^{-1} (KBr): $\nu_{N\equiv O}$ 1878 (vs), ν_{SO} 928, 898 (vs) (dmso-O), ν_{Ru-O} 503, 492 (m). UV−vis spectrum (λ_{max}, nm (ϵ, M^{-1} cm^{-1})): in CH_3NO_2 solution, 498 (v br) (55).

For comparative purposes, the complex was prepared also by the method described in ref 23.

***mer,trans*-RuCl$_3$(dmso-S)(dmso-O)(NO) (3).** A 1.4 g amount of $[(dmso)_2H][trans\text{-}RuCl_4(dmso\text{-}S)_2]$ (2.5 mmol) was dissolved in 15 mL of water and treated with NO for 2 h as described for the preparation of **1**, path b. A small amount of an orange precipitate formed during the reaction. It was collected by filtration, washed with water, cold acetone, and diethyl ether, and vacuum-dried. A further crop of this product was found in the precipitate of **1** and was recovered after dissolution of **1** in water. Yield: 0.14 g (14%). Anal. Calcd for $C_4H_{12}NCl_3O_3RuS_2$ (M_r 393.69): C, 12.2; H, 3.08; N, 3.56. Found: C, 12.3; H, 3.02; N, 3.55.^{1}H NMR spectrum in CD_3NO_2: 2.91 (6, s, dmso-O), 3.55 (6, s, dmso-S). $^{13}C\{^1H\}$ NMR spectrum in CD_3NO_2: 38.7 (dmso-O), 45.3 (dmso-S). Selected IR, cm^{-1} (KBr): $\nu_{N\equiv O}$ 1896 (vs), ν_{SO} 1140 (vs) (dmso-S), 900 (vs) (dmso-O), ν_{Ru-O} 491 (m), ν_{Ru-S} 428 (m). UV−vis spectrum (λ_{max}, nm (ϵ, M^{-1} cm^{-1})): in CH_3NO_2 solution, 433 (v br) (140). Recrystallization of **3** from a DMF/acetone mixture upon slow diffusion of diethyl ether yielded crystals of the substitution product **3a**, in which the dmso-O is replaced by DMF. Selected IR, cm^{-1} (KBr): $\nu_{N\equiv O}$ 1901 (vs), ν_{CO} 1639 (vs), ν_{SO} 1134 (vs) (dmso-S), ν_{Ru-S} 423 (m).

***trans,cis,cis*-RuCl$_2$(dmso-O)$_2$(NO)(NO$_2$) (5).** A 0.2 g amount of *trans*-$RuCl_2(dmso\text{-}S)_4$ (0.41 mmol) was dissolved in 8 mL of CH_2Cl_2, and nitric oxide was bubbled through the solution for 1 h, causing the system to turn from yellow to purple-red. An orange-red precipitate formed within a few hours and was collected by filtration, washed with cold dichloromethane and diethyl ether, and vacuum-dried. Yield: 0.1 g (60%). Anal. Calcd for $C_4H_{12}N_2Cl_2O_5RuS_2$ (M_r 404.24): C, 11.9; H, 2.99; N, 6.93. Found: C, 11.8; H, 2.89; N, 6.71.^{1}H NMR spectrum in CD_3NO_2: 2.84 (6, s, dmso-O), 3.01 (6, s, dmso-O). $^{13}C\{^1H\}$ NMR spectrum in CD_3NO_2: 37.9, 38.7 (dmso-O). Selected IR, cm^{-1} (KBr): $\nu_{N\equiv O}$ 1906 (vs), ν_{NO2} 1431 (s, ν_{as}), 1328 (s, ν_{sym}), ν_{SO} 916 (vs) (dmso-O), δ_{NO2} 825 (m), ν_{Ru-O} 499, 486 (m). UV−vis spectrum (λ_{max}, nm (ϵ, M^{-1} cm^{-1})): in CH_3NO_2 solution, 413 (110). The same product, even though in lower yield (35%) and containing ca. 10% of *mer,cis*-$RuCl_3(dmso\text{-}O)_2(NO)$ (according to ^{1}H NMR spectra), was obtained using *cis*-$RuCl_2(dmso)_4$ as starting material.

[(Im)$_2$H][*trans*-RuCl$_4$(Im)(NO)] (6). A 0.1 g amount of imidazole (1.5 mmol) was added to 0.15 g of $[ImH][trans\text{-}RuCl_4(dmso\text{-}O)(NO)]$ (**1Im**, 0.36 mmol) partially dissolved in 15 mL of acetone; the mixture was refluxed for 3 h, yielding a red solution. Acetone was rotary-evaporated and the resulting red oil redissolved in nitromethane (5 mL); a deep-red microcrystalline precipitate formed within 2 days upon addition of a few drops of diethyl-ether. It was

Table 1. Crystallographic Data for Compounds **1**, **2**, **3a**, **5**, and **6**

	1	**2**	**3a**	**5**	**6**
empirical formula	$C_6H_{19}Cl_4NO_4RuS_3$	$C_4H_{12}Cl_3NO_3RuS_2$	$C_5H_{13}Cl_3N_2O_3RuS$	$C_4H_{12}Cl_2N_2O_5RuS_2$	$C_9H_{13}Cl_4N_7ORu$
fw	508.27	393.69	388.65	404.25	478.13
cryst syst	orthorhombic	monoclinic	triclinic	monoclinic	monoclinic
space group	*Pbca* (No. 61)	$P2_1/n$ (No. 14)	$P\bar{1}$ (No. 2)	$P2_1/c$ (No. 14)	$P\ 2_1/n$ (No. 14)
a, Å	10.402(1)	8.807(2)	7.607(2)	8.827(1)	10.464(3)
b, Å	18.801(4)	11.940(2)	9.692(3)	13.514(1)	11.259(4)
c, Å	19.328(4)	12.824(2)	9.695(3)	11.795(1)	16.095(4)
α, deg			84.90(2)		
β, deg		104.24(2)	91.41(2)	102.958(9)	108.57(2)
γ, deg			68.36(2)		
V, Å^3	3779.9(12)	1307.1(4)	660.5(3)	1371.2(2)	1797.5(9)
D_{calcd},g cm^{-3}	1.786	2.001	1.954	1.958	1.767
Z	8	4	2	4	4
μ (Mo−Kα), mm^{-1}	1.731	2.114	1.940	1.842	1.476
F(000)	2032	776	384	800	944
θ range, deg	2.11−27.10	2.37−29.97	2.93−27.48	2.33−29.97	2.06−27.87
no. reflns collcd	4171	4126	4040	4326	7140
no. indep reflns	4171	3796	2499	3951	4243
R_{int}		0.0402	0.0345	0.0479	0.0251
no. refined params	194	131	199	149	199
GOF (F^2)	0.981	0.938	1.089	1.057	1.099
R1 ($I > 2\sigma(I)$)[a]	0.0448	0.0417	0.0346	0.0414	0.0369
wR2[a]	0.0792	0.0844	0.0885	0.1186	0.0910
residuals, e/Å^3	0.377, −0.527	0.523, −0.837	0.812, −0.470	1.536,[b] −1.270	1.094,[b] −0.354

[a] $R1 = \sum||F_o| - |F_c||/\sum|F_o|$, $wR2 = [\sum w(F_o^2 - F_c^2)^2/\sum w(F_o^2)^2]^{1/2}$. [b] Close to Ru atom.

removed by filtration, washed with cold nitromethane and diethyl ether, and vacuum-dried. The product contains one imidazole molecule of crystallization and is better formulated as [$(Im)_2H$]-[*trans*-$RuCl_4(Im)(NO)$]. Yield: 56 mg (32%). Anal. Calcd for $C_9H_{13}N_7Cl_4ORu$ (M_r 478.13): C, 22.6; H, 2.74; N, 20.5. Found: C, 22.4; H, 2.62; N, 20.1. ^{1}H NMR spectrum in D_2O: 7.23 (1, s, Im), 7.31 (4, s, ImH), 7.56 (1, s, Im), 8.23 (2, s, ImH), 8.39 (1, s, Im). Selected IR, cm^{-1} (KBr): $\nu_{N\equiv O}$ 1873 (vs), (Im) 1064 (s), 652 (s), 619 (s); (ImH) 609 (s). UV−vis spectrum (λ_{max}, nm (ϵ, M^{-1} cm^{-1})): in H_2O solution, 509 (v br) (50).

[TBA][*trans*-$RuCl_4(Im)(NO)$] (6TBA). A 0.05 g amount of imidazole (0.73 mmol) was added to 0.11 g of [TBA][*trans*-$RuCl_4$-(dmso-O)(NO)] (**1TBA**, 0.18 mmol) dissolved in 5 mL of acetone; the mixture was refluxed for 3 h, yielding a red solution. A deep-red microcrystalline precipitate formed upon cooling to ambient temperature; it was removed by filtration, washed with cold acetone and diethyl ether, and vacuum-dried. Yield: 0.036 g (33%). Anal. Calcd for $C_{19}H_{40}N_4Cl_4ORu$ (M_r 583.43): C, 39.1; H, 6.91; N, 9.60. Found: C, 39.6; H, 7.06; N, 9.75.^{1}H NMR spectrum in CD_3NO_2: 0.98 (12, t, TBA), 1.42 (8, m, TBA), 1.73 (8, m, TBA), 3.26 (8, m, TBA), 7.22 (1, s, Im), 7.53 (1, s, Im), 8.34 (1, s, Im). Selected IR, cm^{-1} (KBr): $\nu_{N\equiv O}$ 1861 (vs), (Im) 1064 (s), 654 (s), 619 (s). UV−vis spectrum (λ_{max}, nm (ϵ, M^{-1} cm^{-1})): in CH_3NO_2 solution, 463 (77).

[ImH][*trans*-$RuCl_3(NO_2)(Im)(NO)$] (7). A 0.3 g amount of [ImH][*trans*-$RuCl_4$(dmso-S)(Im)] (0.65 mmol) was dissolved in 10 mL of H_2O, and nitric oxide was bubbled through the solution for 5 h. Water was then rotary-evaporated and the resulting red oil redissolved in nitromethane (3 mL) and stored at 4 °C; a pale-pink precipitate formed within 2 days upon addition of a few drops of diethyl ether. It was removed by filtration, washed with cold nitromethane and diethyl ether, and vacuum-dried. Yield: 20 mg (7%). Anal. Calcd for $C_6H_9N_6Cl_3O_3Ru$ (M_r 420.60): C, 17.1; H, 2.16; N, 20.0. Found: C, 16.9; H, 2.11; N, 18.6. ^{1}H NMR spectrum in D_2O: 7.27 (s, 1, Im), 7.37 (s, 1, Im), 7.46 (s, 2, ImH), 8.21 (s, 1, Im), 8.62 (s, 1, ImH). Selected IR, cm^{-1} (KBr): $\nu_{N\equiv O}$ 1861 (vs), ν_{NO2} 1405 (s, ν_{as}), 1318 (s, ν_{sym}); δ_{NO2} 826 (m), (Im) 1071 (s), 646 (s), 621 (s); (ImH) 1046 (s), 608 (s).

Electrochemistry. All electrochemical experiments were conducted in a dimethylformamide solution containing 0.1 M [TBA]-[BF_4] as supporting electrolyte. In addition, the electrochemical response of complex **3** was also investigated in dimethyl sulfoxide/0.1 M [TBA][BF_4]. The solutions were purged with nitrogen for 20 min prior to study and were kept under an atmosphere of nitrogen throughout the experiments. Cyclic voltammetric experiments employed a Pt disk micro working electrode (0.5 mm diameter), a Pt counter electrode with a large surface area, and a Ag/AgCl reference electrode. Using this experimental setup, the ferrocenium/ferrocene couple is measured at +0.55 V. Unless otherwise stated, all voltammograms were measured at a scan rate of 100 mV s^{-1}. Coulometric experiments were conducted in an H-type cell with a Pt basket working electrode and the other electrodes as before. Electrochemical experiments were recorded using an Autolab system containing a PSTAST30 potentiostat with GPES version 4.8 software. The UV−vis spectra were recorded on a Perkin-Elmer Lambda 19 spectrometer, IR spectra were recorded on a FTIR 2000 Perkin-Elmer spectrometer, and EPR spectra were recorded on a Bruker X-band spectrometer.

X-ray Crystallography. Crystal data, data collections, and refinement parameters for the structures reported are summarized in Table 1. Data sets for **1**, **2**, and **5** were collected at room temperature using $\omega-2\theta$ scan technique on a CAD4 Enraf-Nonius diffractometer, equipped with graphite-monochromator and Mo Kα radiation ($\lambda = 0.71073$ Å). Intensities of three standard reflections were monitored during data collection, and a decrease in intensity of 18.7% for compound **1** was corrected with a linear fit. The reflections were corrected for Lorentz polarization effects and for absorption, based on an empirical ψ-scan method. Data collections for **3a** and **6** were carried out using a Nonius DIP-1030H system with Mo Kα radiation. A total of 30 frames were collected, each with an exposure time of 12 min, over a half of reciprocal space with a rotation of 6° about φ, with the detector at a distance of 80 mm from the crystal. Data reduction and cell refinement was carried out using the program Mosflm.[28]

(28) Collaborative Computational Project, Number 4: *Acta Crystallogr.* **1994**, *D50*, 760−763.

Scheme 1

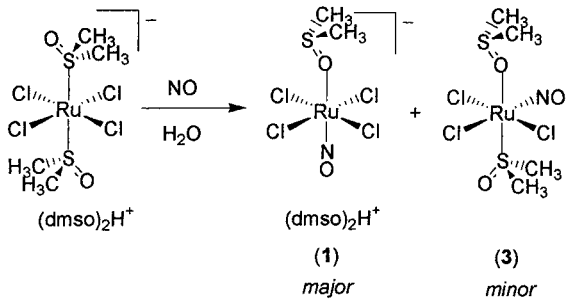

All the structures were solved by Patterson and Fourier analyses[29] and refined by the full-matrix least-squares method based on F^2 with all observed reflections.[30] The final cycles with fixed contribution of hydrogen atoms converged to final R1 and wR2 factors reported in Table 1. All the calculations were performed using the WinGX System, Ver 1.64.02.[31]

Results and Discussion

Synthesis. We first investigated the reactivity of basic ruthenium(II)− and ruthenium(III)−chloride−dimethyl sulfoxide precursors toward nitric oxide by passing NO gas through a solution (or suspension) of the complex. This is the most widely used synthetic procedure for nitrosyl complexes.

Both Ru(III) precursors tested, $[(dmso)_2H][trans\text{-}RuCl_4(dmso\text{-}S)_2]$ and $mer\text{-}RuCl_3(dmso)_3$, were found to react with NO at ambient temperature in a similar way; that is, NO replaces one of the two S-bonded dimethyl sulfoxides trans to one another yielding $[(dmso)_2H][trans\text{-}RuCl_4(dmso\text{-}O)(NO)]$ (**1**) and $mer,cis\text{-}RuCl_3(dmso\text{-}O)_2(NO)$ (**2**), respectively (Schemes 1 and 2). The geometries of the two complexes were confirmed by X-ray analysis (see in a following section).

Preparation of anionic complex **1** could be performed either in nitromethane or in water, while that of neutral compound **2** was best performed in CH_2Cl_2. The imidazolium salt of **1**, $[ImH][trans\text{-}RuCl_4(dmso\text{-}O)(NO)]$ (**1Im**, Im = imidazole), was similarly obtained from the corresponding precursor; the tetra *n*-butylammonium (TBA) salt, $[TBA][trans\text{-}RuCl_4(dmso\text{-}O)(NO)]$ (**1TBA**), which is well soluble in organic solvents, was best prepared from **1** by anion exchange. Interestingly, compounds **1** and **1Im** were obtained in good yields and with shorter reaction times from the corresponding precursors using water, instead of nitromethane, as solvent. The greater reactivity of $[trans\text{-}RuCl_4(dmso\text{-}S)_2]^-$ toward NO in aqueous solution compared to nitromethane was to be expected: while upon dissolution in water $[trans\text{-}RuCl_4(dmso\text{-}S)_2]^-$ immediately dissociates one dmso ligand, thus opening up a coordination site, in nitromethane only partial dissociation occurs according to ^{1}H NMR spectroscopy. Alternatively, complex **1** could be prepared with high yield also by treatment of hydrated $RuCl_3$ with dmso and concentrated HCl in refluxing ethanol.

The IR spectra of **1** and **2**, beside a strong nitrosyl stretching in the region for linear nitrosyls, show S−O stretching bands for O-bonded dmso. The ^{1}H and $^{13}C\{^1H\}$ NMR spectra of compounds **1** and **2** have sharp resonances in the region of O-bonded dmso exclusively (the two dmso-O singlets found in the ^{1}H NMR spectrum of **2** indicate that the two sulfoxides must be in cis position). These spectroscopic features are consistent with the $\{Ru(NO)\}^6$ formulation for **1** and **2**, that is, a diamagnetic Ru^{II} nucleus bound to NO^+. Moreover, coordination of the strong π-acceptor NO induces an S to O linkage isomerization of the dmso trans to it to avoid competition for π-electrons.[32] We had observed a similar behavior when, in the same precursors, dmso-S was replaced by CO.[33]

The electronic spectra of **1** and **2**, characterized by a very broad and weak absorption centered at about 500 nm, are completely different from those of the corresponding precursors, which are dominated by strong and typical charge-transfer bands from the chlorides to Ru(III).[26] This is consistent with the change in oxidation state of ruthenium upon binding of NO. For comparison, formation of $[(dmso)_2H][trans\text{-}RuCl_4(dmso\text{-}O)(CO)]$ and $mer,cis\text{-}RuCl_3(dmso\text{-}O)_2(CO)$ from the corresponding precursors left the shape of the spectra almost unchanged, inducing only a rather large red shift (ca. 50 nm) of the main band.[33]

A complex formulated as $RuCl_3(dmso\text{-}O)_2(NO)$ (nothing was said about its geometry), and characterized by a single ν(SO) at 910 cm^{-1}, was prepared by Fergusson and coworkers by treatment of "$RuCl_3(NO)$" in refluxing dimethyl sulfoxide.[24] In our hands, that synthetic route yielded a product with the same analytical and spectroscopic features as complex **2**. An isomer of compound **2**, labeled as **3**, was isolated in low yield during the preparation of **1** in aqueous solution (Scheme 1); according to spectroscopic evidence, beside coordinated NO, compound **3** has one dmso bound through sulfur and one through oxygen, both with equivalent methyls (singlets at δ = 3.55 and 2.91, respectively). Two geometries, excluding that with dmso-S trans to NO, are compatible with the NMR data, that is, the two $mer\text{-}RuCl_3(dmso\text{-}S)(dmso\text{-}O)(NO)$ isomers, one with NO trans to dmso-O and the other with NO trans to Cl.[34] It seems unlikely that the large difference in the electronic spectra observed between **2** and **3** is caused only by the O to S isomerization of the dmso trans to Cl. Moreover, the NO stretching frequency in **3** is significantly higher than in **2** (20 cm^{-1}), suggesting that the ligand trans to NO in **3** is an overall worse donor of charge density than that in **2**. According to these features, the "NO trans to Cl" geometry seems more likely for isomer **3**; this geometry was confirmed by X-ray analysis (see later). Thus, compound **3** derives from $[trans\text{-}RuCl_4$-

(29) SHELXS-86, Program for structure solution: Sheldrick, G. M. *Acta Crystallogr.* **1990**, *A46*, 467−473.
(30) Sheldrick, G. M. *SHELXL-97, Program for crystal structure refinement*; University of Göttingen: Göttingen, Germany, 1997.
(31) Farrugia, L. J. *WinGX−A Windows Program for Crystal Structure Analysis*; University of Glasgow: Glasgow, U.K., 1998.
(32) S-bonded dmso is generally considered as a mild π-acceptor ligand, see ref 33.
(33) Alessio, E.; Bolle, M.; Milani, B.; Mestroni, G.; Faleschini, P.; Geremia, S.; Calligaris, M. *Inorg. Chem.* **1995**, *34*, 4716−4721.
(34) In the $fac\text{-}RuCl_3(dmso\text{-}S)(dmso\text{-}O)(NO)$ isomer, the two methyl groups on each dmso ligands would be inequivalent, and four resonances are to be expected.

Scheme 2

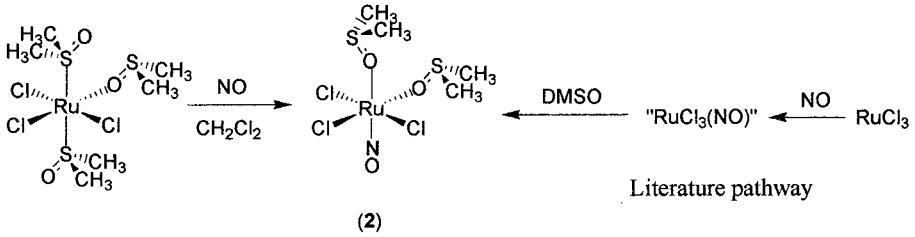

Scheme 3

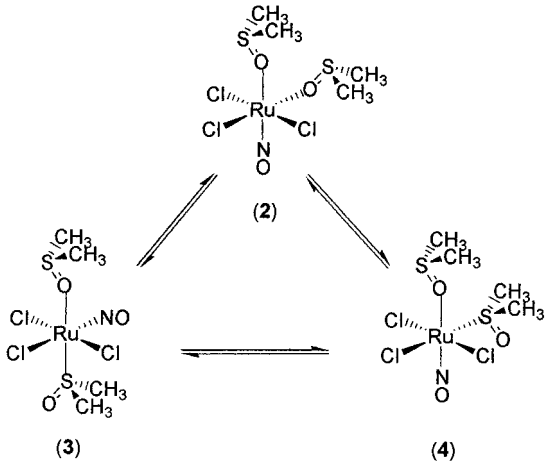

Scheme 4

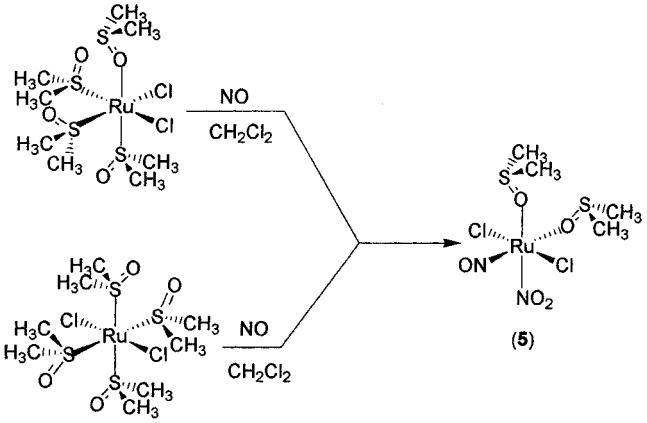

$(dmso\text{-}S)_2]^-$ upon replacement of a chloride by NO, accompanied by the S to O isomerization of one sulfoxide (Scheme 1). Recrystallization of **3** from a DMF/acetone mixture upon slow diffusion of diethyl ether yielded crystals suitable for X-ray diffraction (vide infra) of the substitution product *mer*-$RuCl_3$(dmso-S)(DMF)(NO) (**3a**), in which the dmso-O is replaced by DMF.

Complex **3** is unstable in nitromethane solution; the CD_3NO_2 NMR signals of **3** (light protected solution) are slowly replaced by those of **2** and by two new equally intense singlets, one corresponding to O-bonded ($\delta = 2.93$), and the other, to S-bonded ($\delta = 3.34$) dmso. Such resonances must belong to the other *mer*-$RuCl_3$(dmso-S)(dmso-O)(NO) isomer, that with NO trans to dmso-O (**4**) (Scheme 3). An equilibrium mixture, consisting of ca. 64% **2**, 3% **3**, and 33% **4**, is reached within 1 week at 30 °C, thus indicating that the order of thermodynamic stability of the three isomers is **2** > **4** ≫ **3**. The same equilibrium mixture was reached also from a CD_3NO_2 solution of complex **2** in 2 days at 30 °C. No signal for free dimethyl sulfoxide was observed to grow during these isomerizations.

Treatment of the Ru(II) precursor *trans*-$RuCl_2(dmso\text{-}S)_4$ with gaseous NO in CH_2Cl_2 solution yielded a new product, characterized as the nitrosyl−nitro derivative *trans,cis,cis*-$RuCl_2(dmso\text{-}O)_2(NO)(NO_2)$ (**5**, Scheme 4). According to structural and spectroscopic evidence, this complex can also be formulated as containing the $\{Ru^{II}(NO^+)\}^6$ moiety; electroneutrality of the complex is reached by coordination (through N) of the NO_2^- group. Both dmso ligands in **5** are O-bonded to Ru, implying that also in this case S to O bonded isomerization has occurred. The same product, even though in lower yield and impure for *mer*-$RuCl_3(dmso\text{-}O)_2$-(NO) (**2**), was obtained using the geometrical isomer *cis*-$RuCl_2(dmso)_4$ as starting material (Scheme 4). Examples of nitrosyl−nitro ruthenium complexes can be found in the literature,[15,19,35] and some of them were found to undergo nitro−nitrito thermal or redox-induced linkage isomerization.[15]

In the second part of our synthetic work, we investigated the reactivity of the antimetastatic drug [ImH][*trans*-$RuCl_4$-(dmso-S)(Im)] (NAMI-A) toward NO, with the aim of preparing a reference compound with NO in place of the sulfoxide. We found that coordination of NO to NAMI-A in organic solvents is more difficult than to its precursor and involves replacement of imidazole rather than dmso. Treatment of NAMI-A in nitromethane/dmso mixtures (where it is partially soluble) with NO yielded [ImH][*trans*-$RuCl_4$-(dmso-O)(NO)] (**1Im**) in relatively low yield. The same product was obtained also upon treatment of the corresponding TBA salt, [TBA][*trans*-$RuCl_4$(dmso-S)(Im)], in CH_2Cl_2 solution; this reaction, which involves protonation of coordinated imidazole, occurred also when dehydrated CH_2Cl_2 was used and the presence of oxygen in the system was carefully avoided. Thus, we resolved to prepare the reference compound using [ImH][*trans*-$RuCl_4$(dmso-O)(NO)] (**1Im**) as starting material. However, unlike its precursor or the corresponding CO adduct, [*trans*-$RuCl_4$(dmso-O)(NO)]$^-$ is remarkably inert in nitromethane and aqueous solutions. The D_2O NMR spectrum of **1** remained unchanged for days at ambient temperature, and also, addition of a 5-fold excess of imidazole did not lead to replacement of the O-bonded sulfoxide, which is normally a quite weak and labile ligand. Replacement of dmso-O occurred by treatment of **1Im** with excess imidazole in refluxing acetone (Scheme 5); the

(35) Keene, F. R.; Salmon, D. J.; Walsh, J. L.; Abruña, H. D. *Inorg. Chem.* **1980**, *19*, 1896−1903.

Scheme 5

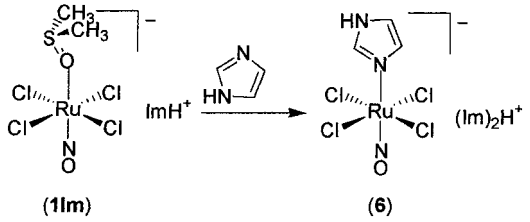

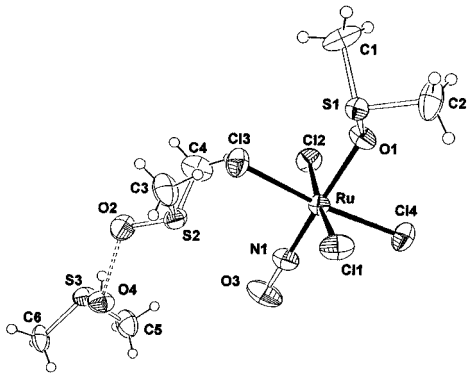

Figure 1. Molecular structure of $[(dmso)_2H][trans\text{-}RuCl_4(dmso\text{-}O)(NO)]$ (**1**) (ORTEP drawing, 40% probability for thermal ellipsoids). Selected bond lengths (Å) and angles (deg): Ru−N(1) 1.712(5); Ru−O(1) 2.029(3); Ru−Cl(1) 2.356(2); Ru−Cl(2) 2.373(2); Ru−Cl(3) 2.365(2); Ru−Cl(4) 2.362-(2); N(1)−O(3) 1.134(5); Ru−N(1)−O(3) 178.0(5); Ru−O(1)−S(1) 123.46-(19).

product contains one molecule of imidazole of crystallization beside the imidazolium cation, and it is thus formulated as $[(Im)_2H][trans\text{-}RuCl_4(Im)(NO)]$ (**6**). The corresponding TBA salt, **6TBA**, was similarly prepared from [TBA][*trans*-$RuCl_4$-(dmso-O)(NO)]. Replacement of dmso-O with imidazole in the position trans to NO leads to no significant change in the NO stretching frequency. Compound **6** is remarkably inert in aqueous solution (its D_2O NMR spectrum remained unchanged for weeks at ambient temperature), and unlike NAMI-A, it remains inert also at physiological pH.

The behavior of NAMI-A toward gaseous NO changes remarkably when the reaction is run in aqueous solution. In this solvent, both dmso and one chloride are slowly replaced, and nitrosyl−nitro complex $[ImH][mer\text{-}RuCl_3(Im)(NO)(NO_2)]$ (**7**) is isolated in low yield. According to the NMR spectrum, raw complex **7** contains a relatively small amount (ca. 15%) of **6**.

Description of the Structures. Figures 1−5 give a perspective view of the molecular structure of compounds **1**, **2**, **3a**, **5**, and **6**.[36] Because of the low quality of the crystals, X-ray analysis of **3** afforded an unambiguous determination of the geometry of the complex but did not allow us to determine meaningful geometrical parameters (*R* value ca. 14%). An attempt to recrystallize it from DMF solution led to the derivative **3a**, where the dmso-O ligand was replaced by a solvent molecule.

In all the complexes, the metal displays the expected octahedral coordination geometry with a linear nitrosyl group

(36) During the preparation of this manuscript, an X-ray structure of complex **2** prepared according to the literature procedure (ref 24) was reported: Paula, Q. A.; Batista, A. A.; Castellano, E. E.; Ellena, J. *J. Inorg. Biochem.* **2002**, *90*, 144−148.

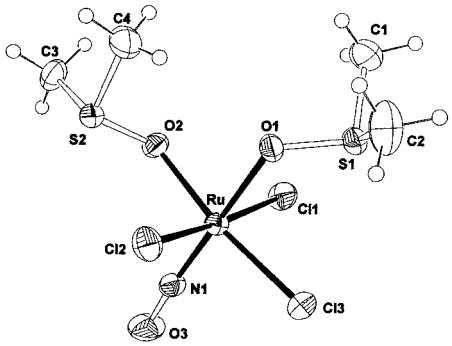

Figure 2. Molecular structure of *mer*,*cis*-$RuCl_3(dmso\text{-}O)_2(NO)$ (**2**) (ORTEP drawing, 40% probability for thermal ellipsoids). Selected bond lengths (Å) and angles (deg): Ru−N(1) 1.704(4); Ru−O(1) 2.035(3); Ru−O(2) 2.076(3); Ru−Cl(1) 2.364(1); Ru−Cl(2) 2.354(1); Ru−Cl(3) 2.335-(1); N(1)−O(3) 1.141(5); Ru−N(1)−O(3) 175.6(4); Ru−O(1)−S(1) 122.43-(17); Ru−O(2)−S(2) 122.80(17).

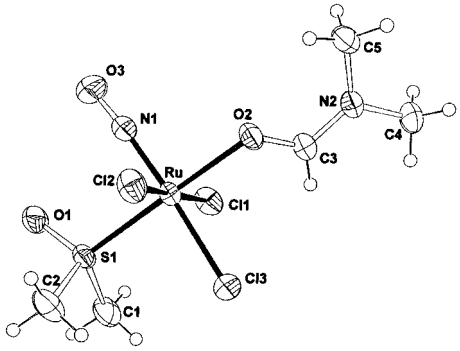

Figure 3. Molecular structure of *mer*-$RuCl_3(dmso\text{-}S)(DMF)(NO)$ (**3a**) (ORTEP drawing, 40% probability for thermal ellipsoids). Selected bond lengths (Å) and angles (deg): Ru−N(1) 1.748(3); Ru−O(2) 2.101(2); Ru−S(1) 2.325(1); Ru−Cl(1) 2.372(1); Ru−Cl(2) 2.373(1); Ru−Cl(3) 2.329-(1); N(1)−O(3) 1.135(4); Ru−N(1)−O(3) 175.2(3).

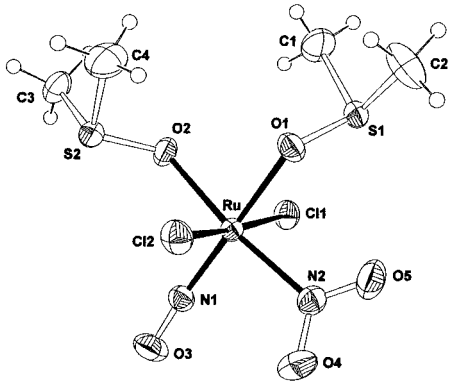

Figure 4. Molecular structure of *trans*,*cis*,*cis*-$RuCl_2(dmso\text{-}O)_2(NO)(NO_2)$ (**5**) (ORTEP drawing, 40% probability for thermal ellipsoids). Selected bond lengths (Å) and angles (deg): Ru−N(1) 1.711(4); Ru−O(1) 2.027(4); Ru−O(2) 2.091(4); Ru−N(2) 2.059(5); Ru−Cl(1) 2.359(1); Ru−Cl(2) 2.357-(1); N(1)−O(1) 1.151(6); Ru−N(1)−O(1) 173.9(2); Ru−O(1)−S(1) 124.7-(2); Ru−O(2)−S(2) 123.5(2).

which is trans to a dmso-O in compounds **1**, **2**, and **5**, to a chloride in **3a**, and to an imidazole ligand in **6**. The Ru−NO bond length of 1.748(3) and 1.740(3) Å in **3a** and **6**, respectively, appears to be longer compared to the values observed in the other complexes (1.712(5)−1.704(4) Å); Ru is invariably displaced by about 0.1 Å from the equatorial mean plane toward NO. The short Ru−NO bond distances are consistent with strong $d_\pi \rightarrow \pi^*$ NO back-bonding and confirm the values usually detected in ruthenium nitrosyl

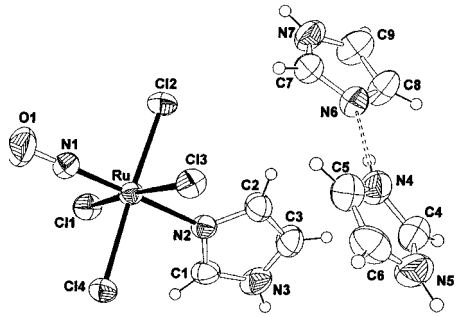

Figure 5. Molecular structure of $[(Im)_2H][trans\text{-}RuCl_4(Im)(NO)]$ (**6**) (ORTEP drawing, 40% probability for thermal ellipsoids). Selected bond lengths (Å) and angles (deg): Ru−N(1) 1.740(3); Ru−N(2) 2.091(2); Ru−Cl(1) 2.376(1); Ru−Cl(2) 2.372(1); Ru−Cl(3) 2.372(1); Ru−Cl(4) 2.380(1); N(1)−O(3) 1.128(4); Ru−N(1)−O(3) 177.7(3).

complexes.[37] The N−O bond lengths fall in a range from 1.128(4) (**6**) to 1.151(6) Å (**5**), a trend not reflected by the N−O stretching frequencies, which do not make any significative difference among the complexes evident.

All the dmso ligands are bound through oxygen with the exception of those in **3** and in **3a**, confirming that in Ru complexes a strong π-acceptor ligand (e.g., CO, NO) favors this coordination mode for the opposing dmso.[33,38]

The only examples of crystal structures containing a sulfoxide−Ru−NO fragment[25] are of low accuracy, and a comparison with the more accurate data reported here gives results that are meaningless. On the other hand, it is worthwhile to compare the present Ru−O bond lengths trans to NO with those found in similar neutral sulfoxide−Ru(II)−CO complexes,[38] in order to assess the effect of the two strong π-accepting ligands on the geometrical parameters.

The Ru−O bond distances trans to NO in **1**, **2**, and **5** (2.029(3), 2.035(3), 2.027(4) Å, respectively) are significantly shorter, by about 0.1 Å, than those observed when the trans ligand is CO, as in *trans*,*cis*,*cis*- and *trans*,*trans*,*trans*-Ru(CO)(dmso-O)(dmso-S)$_2$Cl$_2$ (2.139(5), 2.134(5), and 2.142(8) Å), but are also shorter compared to that of 2.095(4) Å detected in *fac*-Ru(CO)$_3$(dmso-O)Cl$_2$, where three COs compete for the π-back-donation from the metal.[38,39] The same trend is confirmed when the Ru−N bond distance of 2.091(2) Å (trans to NO) in the anion of **6** is compared with that of 2.126(6) Å found in the Ru(III) derivative [*trans*-RuCl$_4$(MeIm)(CO)]$^-$,[40] where the imidazole is trans to CO.

These geometrical features give support to the general belief that NO^+ has a lower σ-donor and a higher π-acceptor strength than the isoelectronic CO, resulting in a global higher electron-acceptor strength for the nitrosyl.[7] The short Ru−O and Ru−N distances trans to NO in **1**, **2**, **5**, and **6** are a further manifestation of the well documented trans-shortening effect exerted by the strongly π-accepting nitrosyl ligand trans to a good σ-donor ligand.[14,41] Accordingly, replacement of the dmso-O trans to NO in **1** requires relatively forcing conditions (see previous description) compared to the similar Ru−CO complexes.[33] Similarly, replacement of coordinated water by Cl^- in the complex [*trans*-Ru(NH$_3$)$_4$(H$_2$O)(NO)]$^{3+}$, where the Ru−O (2.035(5) Å) and Ru−NO (1.715(5) Å) distances are close to the values of the complexes reported in this paper, occurs ca. 30 times slower than in [Ru(NH$_3$)$_5$(H$_2$O)]$^{3+}$, and the pK_a for the water acidity is 3.1, 4 orders of magnitude greater than that of 7.7 found in [*trans*-Ru(NH$_3$)$_4$(H$_2$O)(CO)]$^{2+}$.[21]

Conversely, the Ru−O bond distances trans to Cl in **2** (2.076(3) Å) and trans to NO_2 in **5** (2.091(4) Å) are significantly longer than those observed for the dmso trans to the NO ligand in the same complexes. The Ru−NO_2 bond length in complex **5** (2.059(5) Å) compares well to that of 2.053(8) Å found in the crystal structure of [*cis*-Ru(NO)(NO$_2$)(py-2-carboxylate)$_2$]$^{2+}$, with the NO_2 ligand trans to the carboxyl oxygen.[15]

The stereochemistry of the dmso ligands is characterized by the values of torsion angles Cl−Ru−S−O and Ru−S−O−C. The S(1) atom is oriented toward the midpoint of the chlorines Cl(1) and Cl(3) in **1** and **2**, while the second dmso in **2** shows an eclipsed conformation (Cl(2)−Ru−O(2)−S(2) torsion angle of 2.0(2)°). In complex **5**, the two dmso-O ligands have comparable torsion angles about Ru−O bonds (−20.2(3)° for Cl(2)−Ru−O(2)−S(2) and −11.8(3)° for Cl(1)−Ru−O(1)−S(1)), very likely determined by interligand steric interactions.

All the dmso-O ligands in compounds **1**, **2**, and **5** assume the so-called trans−trans conformation. This is the most favored geometry observed in metal−dmso-O complexes and corresponds to the lowest strain energy, with the Ru−O−S−C angle in the range from −167° to −90°.[42] Correspondingly, in **1**, **2**, and **5**, the Ru−O−S angles fall in a very close range (122.4−124.7°) and appear not to be affected by the stereochemistry observed for the dmso ligands.

Finally, the Ru−Cl bond distances are in the range (2.354(1)−2.380(1) Å) usually observed for Ru(II) complexes, with the exceptions of the shorter values of Ru−Cl(3) in **2** (2.335(1) Å) and in **3a** (2.329(1) Å) where the chloride is trans to a dmso-O and to NO, respectively. The latter bond distance indicates that NO, besides being a strong π-accepting ligand, is a much weaker σ-donor than Cl.

Electrochemistry. The cyclic voltammetric response of complexes **1**, **2**, **5**, and **6** is dominated by an irreversible reduction wave. Figure 6 shows a typical cyclic voltammogram for these complexes, and Table 2 gives the peak potentials of the redox processes for each of the complexes.

(37) Hirano, T.; Ueda, K.; Mukaida, M.; Nagao, H.; Oi, T. *J. Chem. Soc., Dalton Trans.* **2001**, 2341−2345.

(38) Alessio, E.; Milani, B.; Bolle, M.; Mestroni, G.; Faleschini, P.; Todone, F.; Geremia, S.; Calligaris, M. *Inorg. Chem.* **1995**, *34*, 4722−4734.

(39) According to the binding model for dmso, a lengthening of the S−O bond distance is expected upon increasing the M−O bond strength. However, the S−O bond distances observed in complexes **1**, **2**, and **5** (range from 1.536(4) to 1.546(3) Å), despite the corresponding short Ru−O bond lengths, are close to the mean value of 1.538(3) Å reported for O-bonded Ru(II) sulfoxide complexes. See: Calligaris, M. *Croat. Chem. Acta* **1999**, *72*, 147−169.

(40) Batista, A. A.; Olmo, L. R. V.; Oliva, G.; Castellano, E. E.; Nascimento, O. R. *Inorg. Chim. Acta* **1992**, *202*, 37−41.

(41) (a) Veal, J. T.; Hodgson, D. J. *Inorg. Chem.* **1972**, *11*, 1420−1424. (b) Bottomley, F. *J. Chem. Soc., Dalton Trans.* **1974**, 1600−1605. (c) Bottomley, F. *J. Chem. Soc., Dalton Trans.* **1975**, 2538−2541.

(42) Geremia, S.; Calligaris, M. *J. Chem. Soc., Dalton Trans*, **1997**, 1541−1547. Because the two Ru−S−O−C torsion angles are related by the bond angles around the S atom, any geometry can be expressed by just one torsion angle $\varphi 1 = \varphi 2 + 102.9°$.

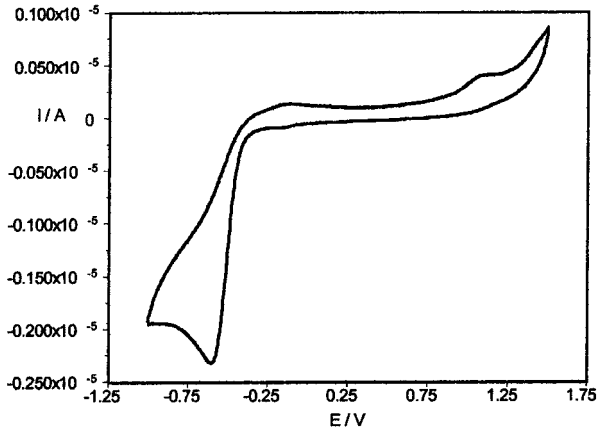

Figure 6. Cyclic voltammetric response for **2** in DMF/0.1 M [TBA][BF_4] at 293 K.

Table 2. Peak Potentials for Complexes **1**, **2**, **3**, **5**, and **6** in DMF/0.1 M [TBA][BF_4] at 293 K

complex	reduction peak potential	daughter products peak potential
1Im	−0.75, −1.25	+1.09
2	−0.59	−0.10, +1.09
3	−0.28, −0.59	
5	−0.51	−0.09
6	−0.74, −0.98	+1.09
6TBA	−0.98	+1.09

Comparison of the electrochemical behavior of **6TBA** and **6** indicates that the redox process at −0.74 V may be assigned to the reduction of the counterion ImH^+. The redox process at −0.75 V in **1Im** may also be assigned to the reduction of ImH^+. The absence of such a peak in **6TBA** indicates that the ligated Im in **6** remains tightly bound to the ruthenium center throughout the electrochemical investigation. The reduction processes at −1.25, −0.59, −0.51, and −0.98 V in **1**, **2**, **5**, and **6**, respectively, are all assigned to the reduction of the NO^+ group bound to Ru(II).[9a,18,43] Previous electrochemical studies of Ru−NO containing compounds have observed the reversible reduction of the NO^+ group at more positive potentials. For example, the one electron reduction of coordinated NO^+ in $[Ru(NH_3)_4L(NO)]^{3+}$ complexes is between −0.36 and −0.13 V vs the SCE,[18] and in [*trans*-RuCl(NO)(cyclam)]$^{2+}$ (cyclam = 1,4,8,-11-tetraazacyclotetradecane), at −0.320 V vs Ag/AgCl.[9a] The more negative reduction potentials measured in this study are a result of replacement of N σ-donor ligands by π-donor Cl^- ligands. The reduction potential for **1** is more negative than that of **6** which suggests that ligated dmso-O is a stronger σ-donor than ligated imidazole. Compounds **2** and **5** contain only three negatively charged ligands as compared to four in compounds **1** and **6** which is reflected in the more positive reduction potentials for **2** and **5**. Exchanging a chloride ligand for a nitro ligand between **2** and **5** results in a slight positive shift in reduction potential because the nitro function is a stronger electron withdrawing group than chloride.[43]

The reduction of the ligated NO group is accompanied by a rapid chemical reaction; hence, there is no sign of a return wave even at low temperature (−50° C) and scan rates up to 5 V s^{-1} for all compounds studied. In all cases, a plot of peak current versus the square root of the scan rate gave a straight line indicating that the electron-transfer process is diffusion controlled. Application of a switching potential more negative than the NO^+-based reduction process results in new redox peaks in the cyclic voltammogram. The potentials of the daughter products generated as a result of reduction of the compounds are given in Table 2. Free chloride is oxidized under the experimental conditions used at +1.09 V. Thus, reductions of compounds **1**, **2**, and **6** are all accompanied by loss of chloride from the compound. Compound **5** showed no loss of chloride ligands as evidenced by no redox process at +1.09 V.

Controlled potential coulometry confirmed that the redox process at −0.59 and −0.51 V in **2** and **5**, respectively, involved one electron. One electron reduction of **2** and **5** resulted in the solution darkening in color. No discernible bands in the visible spectrum could be detected although a broad shoulder at 492 nm is observed in the reduced spectrum of **5**. The NO stretching frequency was monitored throughout the one-electron electrolysis. Initially, ν_{NO} was observed at 1868 and 1887 cm^{-1} for **2** and **5**, respectively, in DMF/0.1 M [TBA][BF_4]. As the electrogeneration proceeded, the NO band decreased in intensity, remaining at the same energy, and disappeared completely after 1 mol equiv of electrons had been passed. No other bands grew in this region of the spectrum during the electrolysis experiment. However, on completion of the electrolysis, a cyclic voltammogram of the resultant solution revealed the presence of 1 mol equiv of chloride ions for **2**, but no such peak was observed after the one electron reduction of **5**. Fast scan cyclic voltammetry at 223 K gave rise to an irreversible anodic peak at −0.1 V for both compounds **2** and **5**. At 293 K, there is only a very small peak at this potential. The mechanism shown in Scheme 6 accounts for all experimental observations.

Scheme 6

$$[RuCl_2(dmso\text{-}O)_2(NO)L] + e^- \rightarrow [RuCl_2(dmso\text{-}O)_2(NO^\bullet)L]^- \quad E_1 \quad (1)$$

$$[RuCl_2(dmso\text{-}O)_2(NO^\bullet)L]^- + DMF \rightarrow [RuCl_2(dmso\text{-}O)_2(NO^\bullet)DMF] + L \quad (2)$$

$$[RuCl_2(dmso\text{-}O)_2(NO^\bullet)DMF] - e^- \rightarrow [RuCl_2(dmso\text{-}O)_2(NO)DMF]^+ \quad E_2 \quad (3)$$

$$[RuCl_2(dmso\text{-}O)_2(NO^\bullet)DMF] + DMF \rightarrow [RuCl_2(dmso\text{-}O)_2(DMF)_2] + NO^\bullet \quad (4)$$

In step 1, compounds **2** and **5** are reduced at E_1, where L = Cl^-, E_1 = −0.59 V and where L = NO_2^-, E_1 = −0.51 V. In both complexes, the site of reduction is the NO group giving the $NO^\bullet$ radical ligand. The reduced complexes are unstable and substitute a negatively charged ligand, L, with a neutral solvent DMF molecule. A similar redox induced

(43) Mondal, B.; Paul, H.; Puranik, V. G.; Lahiri, G. K. *J. Chem. Soc., Dalton Trans.* **2001**, 481−487.

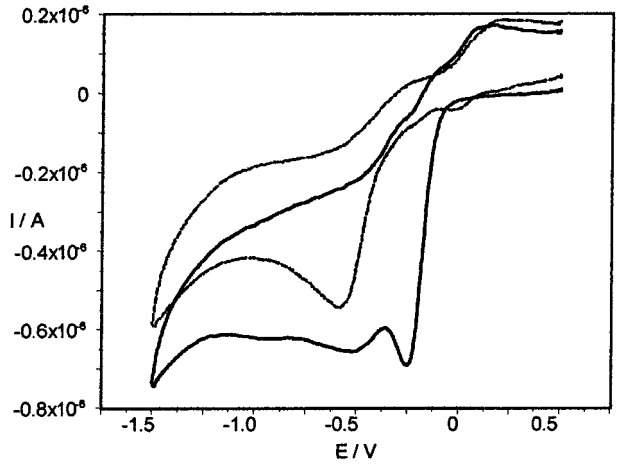

Figure 7. Cyclic voltammetric response for **3** in DMSO/0.1 M [TBA][BF_4] at 293 K, solid line prior to electrogeneration, dashed line after bulk electrosynthesis at −0.32 V.

substitution reaction has been observed in the related compound [*trans*-RuCl(NO)(cyclam)]$^{2+}$.[9a] Step 2 results in the same complex [$RuCl_2$(dmso-O)$_2$(NO$^\bullet$)DMF] being formed which may be oxidized at $E_2 = -0.1$ V. The complex [$RuCl_2$-(dmso-O)$_2$(NO$^\bullet$)DMF] is also unstable and loses NO$^\bullet$ to give the redox inactive compound [$RuCl_2$(dmso-O)$_2$(DMF)$_2$]. None of the solutions were EPR active even at 233 K; very likely, the lifetime of the radical intermediates is too short to be characterized by EPR spectroscopy.

The electrochemical response for complex **3** is very different from that of **1**, **2**, **5**, and **6**. The cyclic voltammogram for **3** in DMSO/0.1 M [TBA][BF_4] is shown in Figure 7 (continuous trace), and the peak potentials are given in Table 2. Two irreversible reduction processes are observed with peak potentials at −0.28 and −0.59 V. Initially, the electrochemical studies on **3** had been conducted in DMF/0.1 M [TBA][BF_4] as for the other complexes investigated. However, concern that **3** may not be stable in DMF (vide supra) led us to repeat the study in DMSO. There was no difference in the redox behavior of **3** in the two solvent systems. Therefore, over the time scale of the electrochemical experiment (ca. 3 h), complex **3** is stable.

Addition of 1 mol equiv of electrons to **3** in either DMF/0.1 M [TBA][BF_4] or DMSO/0.1 M [TBA][BF_4] at −0.32 V resulted in the loss of the cyclic voltammetric wave at −0.28 V. Only the irreversible wave with a peak potential of −0.59 V is visible after electrolysis, see Figure 7 (dashed trace). There is no indication of free chloride in the solution; that is, there is no cv wave at +1.09 V. Bulk electrolysis of this solution at −0.95 V gives no electrochemical response apart from an irreversible wave at +1.09 V typical of free chloride. The initial solution of **3** in either DMF or DMSO has a strong ν_{NO} peak at 1885 cm^{-1}. After electrolysis at −0.32 V, the NO stretching vibration shifts to 1866 cm^{-1}. Further electrolysis at −0.95 V results in complete collapse of this peak. All solutions of **3**, irrespective of electrosynthesis potential, were EPR silent.

We can rationalize the observed electrochemical response of **3** as follows. The site of redox activity in **3** is once again the ligated NO$^+$ group. The NO$^+$ group is trans to Cl$^-$ in **3** which is responsible for the significantly higher NO stretching frequency compared to **2** (vide supra). As has previously been observed,[18] a shift to higher energy for ν_{NO} is accompanied by a shift in the reduction potential to more positive potentials. Thus, we suggest the NO$^+$ group is reduced at −0.28 V on **3** to NO$^\bullet$. This reduction is followed rapidly by an isomerization reaction yielding either **2** or **4** in which the coordinated NO is now trans to a dmso ligand. Thus, the NO$^\bullet$, being electron rich, will not wish to be trans to the π-donating chloride ligand, and hence, the complex isomerizes. The peak potential and the NO stretching frequency of isomerized **3** are very similar to those of **2**. However, the electronic character of **4** is expected to be very similar to that of **2**. The electrogeneration potential of −0.28 V is not negative enough to reduce **2** or **4**, and hence, **3** once reduced and isomerized will immediately oxidize back to NO$^+$. The independence of this process on solvent would indicate that the dmso ligands remain bonded to the Ru^{II} center throughout. The speed of the electrochemically induced isomerism is fast and hence suggests an intramolecular, nondissociative, process.[44] The redox behavior of electrogenerated **2** or **4** is then as described previously.

Reduction of complexes **1** and **6** involved more than 5 electrons and resulted in gross degradation of the solution. Characterization of a solution of **1** or **6** after 1 mol equiv of electrons had been transferred showed a large chloride peak at +1.09 V and the disappearance of the ν_{NO} stretching vibration (in DMF, $\nu_{NO} = 1841$ and 1848 cm^{-1} for **1** and **6**, respectively). No further mechanistic studies were carried out on complexes **1** and **6**.

Conclusions

We prepared and characterized several new ruthenium dimethyl sulfoxide nitrosyls by treatment of basic Ru(II) and Ru(III)−chloride−dimethyl sulfoxide precursors with NO: [(dmso)$_2$H][*trans*-$RuCl_4$(dmso-O)(NO)] (**1**), *mer*,*cis*-$RuCl_3$-(dmso-O)$_2$(NO) (**2**), its isomer *mer*-$RuCl_3$(dmso-S)(dmso-O)(NO) (**3**, with NO trans to Cl) and the DMF substitution product *mer*-$RuCl_3$(dmso-S)(DMF)(NO) (**3a**), and the nitrosyl−nitro derivative *trans*,*cis*,*cis*-$RuCl_2$(dmso-O)$_2$(NO)-(NO_2) (**5**). Alternatively, both **1** and **2** could be prepared with high yield by treatment of hydrated $RuCl_3$ with dmso. Coordination of the strong π-acceptor NO induces an S to O linkage isomerization of the dmso trans to it to avoid competition for π-electrons. Moreover, [(Im)$_2$H][*trans*-$RuCl_4$-(Im)(NO)] (**6**) was prepared by treatment of [ImH][*trans*-$RuCl_4$(dmso-O)(NO)] (**1Im**) with an excess of imidazole in refluxing acetone. The spectroscopic features are consistent with the {Ru(NO)}^{6} formulation for all complexes, that is, a diamagnetic Ru^{II} nucleus bound to NO$^+$.

Compounds **1**, **2**, **3a**, **5**, and **6** were characterized also by X-ray crystallography. All complexes show a linear nitrosyl group, with short Ru−NO bond distances consistent with a strong $d_\pi \rightarrow \pi^*$ NO back-bonding. The Ru−X bond distances trans to NO (X = O in **1**, **2**, and **5**; X = N in **6**) are

(44) Pomeroy, R. K.; Vancea, L.; Calhoun, H. P.; Graham, W. A. G. *Inorg. Chem.* **1977**, *16*, 1508−1514.

remarkably short, in accordance with the well documented trans-shortening effect exerted by the strongly π-accepting nitrosyl group trans to a good σ-donor ligand.[14,41] Correspondingly, an unusual inertness for the O-bonded dmso in compound **1** was found.

Complexes **1**, **2**, **3**, **5**, and **6** are all redox active in DMF solutions showing irreversible reductions whose peak potentials depend on the other ligands attached to the Ru metal center. The site of reduction is the NO^+ moiety. The reduced complexes are not stable and release a Cl^- or NO_2^- ligand followed by the $NO^\bullet$ radical. The initial reduction of **3** is followed by a rapid isomerization to give **2** or **4**. The chemical reactions following electron transfer are all fast (rate constant $> 100\ s^{-1}$ at 293 K). The Ru product species are not redox active within the DMF window.

The purpose of this work was to prepare well characterized ruthenium−dmso−nitrosyls to be used as reference compounds in subsequent biomimetic studies in physiological conditions aimed at understanding whether the anticancer activity of some ruthenium−dmso complexes might be due to their in vivo interactions with NO. The antimetastatic drug [ImH][*trans*-$RuCl_4$(dmso-S)(Im)] (NAMI-A, Im = imidazole) was found to react less promptly toward NO compared to ruthenium−chloride−dmso compounds; however, the reaction conditions used in our synthetic procedures are rather far from those found in physiological solutions.

Acknowledgment. This work is a contribution from the Edinburgh Protein Interaction Centre (EPIC) funded by the Wellcome Trust. We acknowledge finacial support by the Ministero dell'Università e della Ricerca Scientifica (MURST) and by the Regione Autonoma Friuli-Venezia Giulia (L. R. 3/98). Johnson Matthey is gratefully acknowledged for a generous loan of hydrated $RuCl_3$.

Supporting Information Available: X-ray crystallographic file, in CIF format. This material is available free of charge via the Internet at http://pubs.acs.org.

IC011291V